Intruder features in the island of inversion: The case of ^{33}Mg

S. Nummela,[1] F. Nowacki,[2] P. Baumann,[3] E. Caurier,[3] J. Cederkäll,[4] S. Courtin,[3] P. Dessagne,[3] A. Jokinen,[1,5] A. Knipper,[3] G. Le Scornet,[4,6] L. G. Lyapin,[7] Ch. Miehé,[3] M. Oinonen,[4] E. Poirier,[3] Z. Radivojevic,[1] M. Ramdhane,[8] W. H. Trzaska,[1,5] G. Walter,[3] J. Äystö,[1,4] and the ISOLDE Collaboration

[1]*Department of Physics, University of Jyväskylä, P.O. Box 35, Jyväskylä, Finland*

[2]*Theoretical Physics Laboratory, F-67084 Strasbourg Cedex, France*

[3]*IReS, IN2P3-CNRS, Louis Pasteur University, BP 28, F-67037 Strasbourg Cedex, France*

[4]*EP-Division, CH-1211 Geneva, CERN, Switzerland*

[5]*Helsinki Institute of Physics, University of Helsinki, Finland*

[6]*CSNSM, 91405 Campus Orsay, France*

[7]*Khlopin Radium Institute, St. Petersburg, Russia*

[8]*University of Constantine, Constantine, Algeria*

(Received 16 May 2001; published 18 October 2001)

The ^{33}Na β decay was studied online using mass separation techniques and a first description of the level structure of the neutron-rich isotope ^{33}Mg, with $N=21$, has been obtained. The experiment involved the measurement of β-γ, β-γ-γ, and β-n-γ coincidences as well as neutron spectra by time-of-flight technique. The first low energy level scheme for the daughter nucleus ^{33}Mg is given with five bound states. Spin and parity assignments are proposed according to β feedings and γ-ray multipolarities. β-strength distribution is evaluated, taking into account $1n$- and $2n$-emission channels and it is compared with the calculated GT strength distribution. In particular, the $1p$-$1h$ and $2p$-$2h$ excitations are shown to result in substantial contribution to the low energy configurations. Allowed β branch to the ^{33}Mg g.s. [$\log ft=5.27(26)$] gives direct evidence for the inversion of $\nu(f_{7/2})$ and $\nu(d_{3/2})$ states.

DOI: 10.1103/PhysRevC.64.054313 PACS number(s): 21.60.Cs, 23.40.Hc, 27.30.+t, 23.20.Lv

I. INTRODUCTION

The first signs, indicating the inversion in shell ordering at $N=20$, were observed as irregularities in the binding energies of neutron-rich $A\cong 32$ nuclei [1]. Theoretical calculations, both Hartree-Fock [2] and shell model [3–6], were able to reproduce this unexpected increase of binding energy by allowing neutron excitations from the *sd* into the *fp* shell, which lead to deformed ground-state configurations. This particular region of deformation, the so-called island of inversion, has now become accessible through many experimental methods. Out of these, Coulomb excitation has allowed a systematic study of $B(E2;0_1^+\rightarrow 2_1^+)$ values for even Si nuclei [7], as well as for few other close-by nuclei at the borders of the island of inversion [8,9]. Also, recent mass measurements for neutron-rich $29<A<47$ nuclei have revealed a similar effect around $N=28$, where prolate deformations of the ground state are predicted [10]. Another powerful method to study the detailed structure of neutron-rich nuclei is the β decay. In our earlier work [11] we used this method to determine the level schemes of ^{34}Si($N=20$) and ^{35}Si($N=21$) of which the latter provided new information on the evolution of neutron orbits outside the $N=20$ closed shell. These two nuclei have, as expected, a ground-state configuration with a main $0p$-$0h$ component.

In the present study we have advanced one step further and aim to determine the low-energy level scheme of ^{33}Mg($N=21$) via the β decay of ^{33}Na. Now we enter the island of inversion [5,6] where predictions using a simple shell model are no longer valid since $2p$-$2h$, $1p$-$1h$, and $0p$-$0h$ configurations are in close competition at low energy. The ^{33}Na$\rightarrow$^{33}Mg decay has been observed already in 1984 [12,13], however, no information on the decay scheme, or on the level scheme of ^{33}Mg, has been available up to now.

Apart from interest in the shell structure there is also an interest related to the vicinity of the neutron drip line. New efforts have been made to redefine the limit of particle stability in the $N=21$ region. Recent mass evaluations [14] predict ^{31}Ne unbound, while the finite-range droplet model (FRDM) [15] predicts the stability of ^{31}Ne in agreement with an experimental result [16]. ^{31}Ne is expected to be the lightest bound $N=21$ isotone since clear evidence for the instability of ^{30}F has been reported [17], while ^{31}F with 22 neutrons was recently observed [18].

In this paper we present β-γ measurements on ^{33}Na sources and we compare the results with those of shell model calculations. The analysis of the β-delayed neutron emission, registered in the same experiment and the results of which are used in our discussion, are presented in a separate paper [19].

II. EXPERIMENTAL PROCEDURES

The ^{33}Na activity was produced in fragmentation reactions by 1.4 GeV protons, provided by the PS/Booster at CERN, impinging on a uranium carbide target. The target (46 g/cm^2 for U) and its temperature (above 2000 °C) were selected in order to optimize the release of activities with short half-lives. The intensity of the primary beam was 3×10^{13} protons/pulse and the interval between pulses was a multiple of 1.2 s. A typical average yield for ^{33}Na was 2 atoms/s. The reaction products were ionized by a surface-ionization source, accelerated and mass separated by the

ISOLDE facility. During the first 20 ms, starting from each proton pulse, the separator beam gate was open and ions were transported to the experimental setup on to a collection tape. For the remaining time until the next arriving proton pulse the separator beam was deflected off in order to optimize the collection of only the short-living components and to obtain a pure decay period for half-life determination. In order to reduce the amount of contaminants and longer-lived daughter activities, the tape was moved periodically. For detection, we adopted a similar setup as in our previous study of the ^{34,35}Al decays [11]. The collection point was surrounded by a thin plastic scintillator detector, covering about 70% of the total solid angle. This provided a trigger signal for β-γ coincidences and a start signal for the neutron time-of-flight measurements. γ rays were detected with two large-volume Ge detectors allowing to record both β-γ and β-γ-γ coincidences. Furthermore, due to the large energy window for β-delayed neutrons in the ^{33}Na decay, neutron detection played an important role. In fact, more than 20 MeV is available for the β decay of ^{33}Na, out of which only 2.07 MeV corresponds to particle-bound levels in ^{33}Mg. Therefore, eight low-threshold neutron detectors [20] of 15% intrinsic efficiency were located around the collection point [19], with a flight path of 50.8 cm. Neutrons were detected as β-n coincidences to obtain neutron time-of-flight spectra. In some cases, β-n-γ coincidences could be detected as well.

III. RESULTS

Primary identification of γ rays belonging to the ^{33}Na decay was possible as the ^{33}Na lifetime [$T_{1/2}=8.2(4)$ ms, [12]] is short compared to the daughter isotopes ($^{31-33}$Mg) and contaminants, such as multiply-charged ions (e.g., ^{198}Bi,$q=6^+$). Since the decay of ^{33}Na consists of several decay channels, including pure β and β-delayed one-, two-, and even three-neutron decays, an important parameter in the analysis was the time of detection of a β-γ or β-n event. A half-life measurement, performed from β, γ and delayed neutron activities, resulted in an average value, $T_{1/2}=8.0(3)$ ms, in good agreement with the reported one [12]. In Fig. 1 two β-gated γ spectra are presented for $A=33$, corresponding to two time windows relative to the proton pulse. The first spectrum corresponds to a time interval up to 50 ms after the arriving protons pulse [(1a)] and the second corresponds to the following 50–500 ms [(1b)]. Clearly only the first spectrum contains γ rays from the ^{33}Na decay.

Altogether, 19 γ transitions could be assigned to the β decay of ^{33}Na based on the decay rate of their intensity. Six have been reported in Ref. [12], out of which four are deexcitations in ^{33}Mg and two in ^{32}Mg. All transitions, observed in the first time window of this measurement, are listed in Table I together with the information on coincident lines. In this table there are five γ transitions following the β-delayed $1n$ emission, thus belonging to the level scheme of ^{32}Mg [21–23]. Among them, the 885 keV line is the most intense one and corresponds to the known $2_1^+ \rightarrow 0_1^+$ transition. This transition was clearly observed in coincidence with neutrons. Three γ transitions belong to the ^{31}Mg level scheme [23] and correspond to β-delayed $2n$ emission. All three were seen in coincidence with neutrons, although two of them weakly. Special attention should be paid to the 221 keV transition which can be partly explained by a transition in ^{31}Mg but is also related to the ^{33}Mg and ^{32}Al level schemes as it results from coincidences observed with 484 and 735 keV, respectively. The latter has been observed previously [24,25].

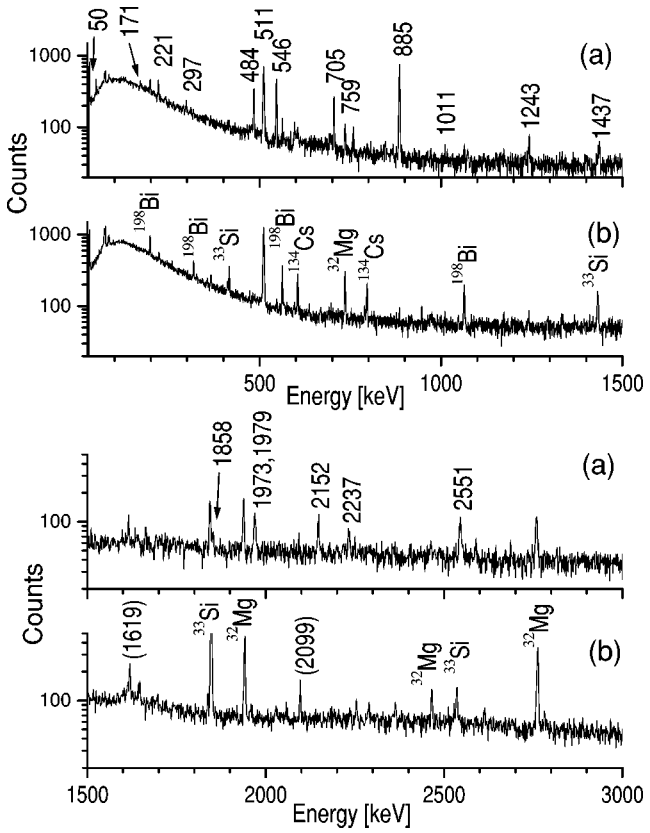

FIG. 1. Gamma spectra measured during the first 50 ms (a) and the next 450 ms (b) after a proton pulse.

Out of the remaining 11 γ rays 6 are used for building the level scheme of ^{33}Mg. All these transitions, except the 546 keV one, are placed in the scheme according to γ-γ coincidence data or according to the sum of γ ray energies. The 546 keV γ transition is the second most intense transition belonging to the ^{33}Na decay scheme, but it cannot be associated to any other transition on the basis of coincidences or energy balance. Its origin could be explained by three possible choices. First, it could de-excitate a level at 546 keV. Second, it could correspond to a de-excitation of one of the levels established through γ-γ coincidences, but with a cascade γ transition outside our observation limits (time or energy). Third, it could belong to the ^{32}Mg level scheme, related to β-delayed $1n$ emission. The third hypothesis can be ruled out as this strong line has not been observed in coincidence with neutrons in our experiment and it was not seen in previous experiments on ^{32}Mg [7,23]. Therefore, only the first two assumptions for the 546 keV placement in the level scheme will be discussed later.

In order to evaluate the β branchings of the ^{33}Na decay to ^{33}Mg, absolute γ intensities together with the P_n values had to be determined. For the evaluation of absolute γ-transition

TABLE I. Energy and intensity of the γ rays attributed to the ^{33}Na decay.

Energy (keV)	Intensity[a] (relative)	Transitions from	Transitions to	Coincidences
50.1 (2)	8.2 (9)	c		
171.2 (1)	3.5 (4)	c		
221.0 (1)	8.7 (10)	705	484	484
	1.4 (2)[d]	c		
297.9 (1)	4.0 (4)			
484.1 (1)	18.7 (19)	484	0	758
546.2 (1)	40.2 (41)	(705)	(159)	
704.9 (1)	23.2 (21)	705	0	
758.2 (1)	6.1 (7)	1243	484	
845.7 (2)	2.5 (4)			
885.3 (1)	100	b		
1011.3 (2)	1.6 (4)			
1242.8 (2)	7.1 (19)	1243	0	
1437.0 (3)	4.7 (8)	b		
1857 (4)	4.1 (6)			
1972.9 (5)	5.9 (10)	b		
1976.9 (5)	6.7 (19)			
2152.4 (1)	10.3 (21)	b		
2236.9 (5)	6.98 (88)			
2551 (1)	16.1 (17)	b		

[a]Intensities are relative to the 885 keV γ ray. The intensity per 100 β decays is obtained by multiplying by a factor 0.22(8).

[b]Corresponding to transitions in the ^{32}Mg level scheme following $1n$ emission.

[c]Corresponding to transitions in the ^{31}Mg level scheme following $2n$ emission.

[d]γ line observed in the second time window (50–500 ms), corresponding to a transition in the ^{32}Al level scheme following $1n$ emission.

intensities, a use was made of the opportunity to measure, with the same setup and in the same experiment, the activity of a well-known β emitter ^{26}Na. This procedure has already been used previously and is described in Ref. [26]. Then, with a ^{33}Na beam collected at the same position, β-multiscaling and γ-ray energy spectra are simultaneously recorded and the ^{33}Na contribution clearly separated from competing activities. Using the ratio of β and γ efficiencies obtained with ^{26}Na, we obtain, after introducing corrections for the differences in γ-ray energy, the absolute intensity of the transitions associated with ^{33}Na.

The β-delayed neutron emission probability of ^{33}Na could not be directly determined from γ intensity analysis only because the decay scheme of ^{33}Mg and ^{33}Al are still unsettled and also because in our experiment the direct production of ^{33}Al from the target is not negligible. Intensities of the γ transitions in ^{33}Mg were compared with those of γ transitions following the β decay of the daughter activities ^{32}Al(1941 keV) and ^{31}Mg(947 keV). An upper limit for the P_n value could be evaluated by comparing the γ intensities in the β-delayed neutron branch and in the direct β decay

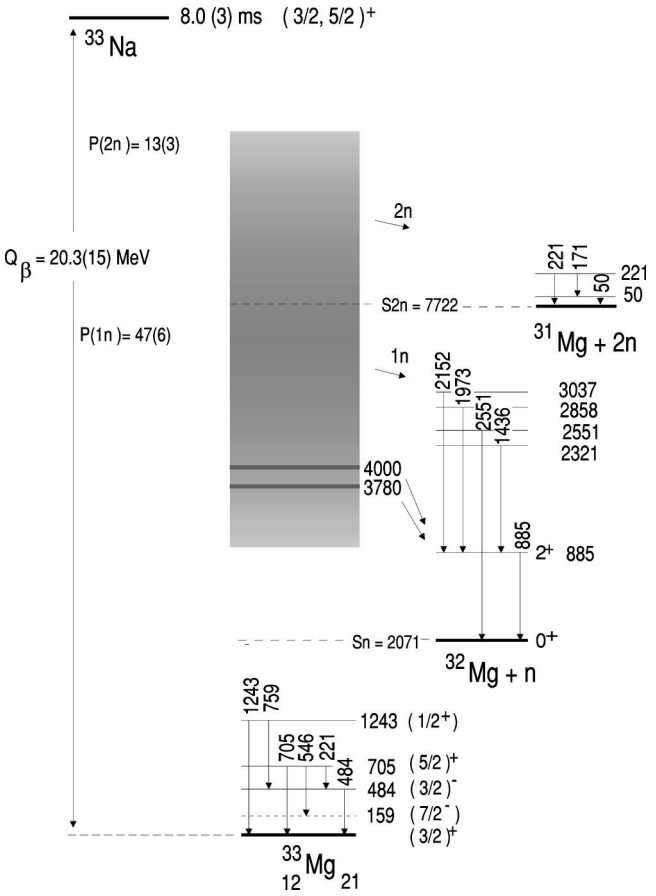

FIG. 2. Experimental decay scheme for ^{33}Na. Reported values for the energy of the levels and relative intensity in the different channels are from the present work and from the analysis of the neutron activity reported in Ref. [19]. J^π values indicated for ^{33}Mg levels, correspond to most plausible values according to beta feedings and gamma intensities (see text). Q_β value is from Ref. [14].

channel. It resulted in the total P_n less than 86% with $P_n = P_{1n} + 2P_{2n}$. For more specific P_n analysis, the P_{1n}/P_{2n} ratio was determined from the relative ^{32}Al and ^{31}Mg activities, resulting in 3.6(9). The determination of the P_n value could be done with independent β and neutron measurements by comparing the absolute β and β-coincident activities. The details of this analysis are described in Ref. [19]. The total neutron emission probability resulted in $P_n = 73(6)\%$. Finally, the absolute P_{1n} and P_{2n} values were obtained from the P_{1n}/P_{2n} ratio, resulting in 47(6) and 13(3) %, respectively. The previously reported values in Ref. [12] are $P_{1n} = 52(20)$ and $P_{2n} = 12(5)$ and thus corroborated by our more precise data.

The decay scheme of ^{33}Na is given in Fig. 2. For all transitions placed in ^{33}Mg, except for the 546 keV one, supporting evidence is provided by the γ-γ coincidences. The difficulty to assign the strong 546 keV line in the level scheme required additional steps. Its decay rate was carefully measured [$T_{1/2} = 7.7(0.9)$ ms] and found in excellent agreement with the ^{33}Na half-life. As mentioned previously, the absence of neutron-γ coincidences rules out attribution to $A = 32$ or 31. Consequently, there are two possible interpretations for the 546 keV transition. First of all, if this transi-

TABLE II. β intensities and logft values in the ^{33}Na β decay to bound levels in ^{33}Mg.

E_x (keV)	I_β (%)	log*ft*
0	20 (10)	5.27 (26)
158.7(1)	a	
484.1(1)	<1.2	>6.6
705.03(9)	15.9 (6.2)	5.20 (22)
1242.7(1)	2.9 (1.2)	5.97 (25)

[a]The feeding of this level is assumed to be neglible, see text.

tion would originate directly from a postulated level at 546 keV, it should be preceded by an allowed GT transition that, according to the intensity analysis, is also the case for the levels at 705 and 1243 keV. However, there are no connecting transitions observed between this hypothetical 546 keV level and the other two mentioned here which have the same parity and for which the angular momentum difference ΔJ should be low. As there are no reasonable explanations why these transitions should be inhibited, or beyond our observation, this interpretation is very unlikely.

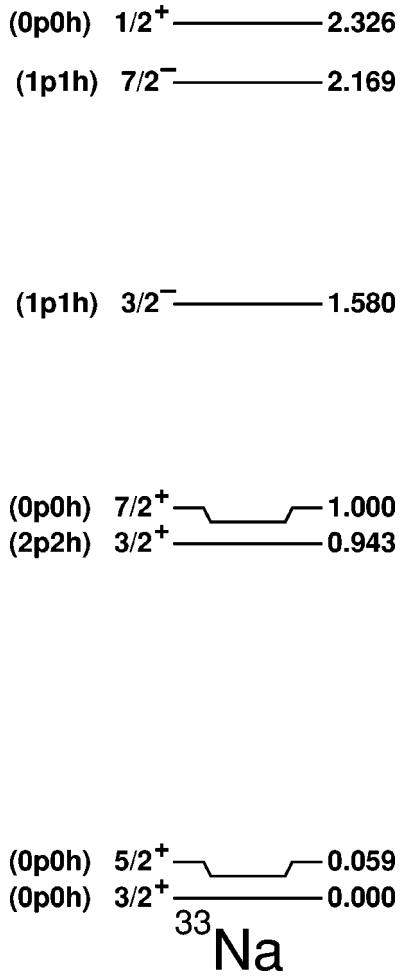

FIG. 3. Calculated low-lying states of ^{33}Na. The indicated *npnh* correspond to a neutron excitation of the core, to be coupled to the odd nucleon.

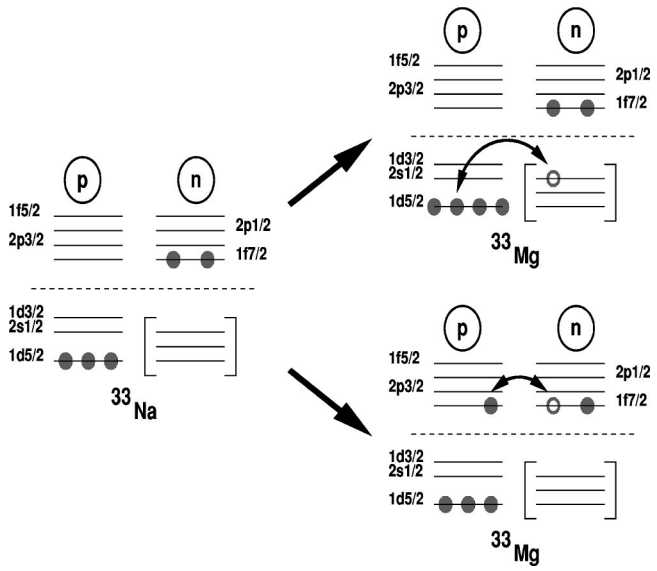

FIG. 4. ^{33}Na allowed Gamow-Teller transitions.

In the remaining alternative, the 546 keV would be associated with an unobserved transition in the decay of one of the other levels validated by γ-γ coincidences, 1243 or 705 keV. Let us first discuss the case of the 1243 keV level. In order to include the 546 keV transition in its decay, an unobserved transition of 697 keV is needed. Yet, at this energy, any transition with $\Delta J \leqslant 2$, even with a change of parity, would satisfy the timing and energy requirements of our experiment. The last possibility is then to associate the 546 keV transition with the decay of the level at 705 keV. This fixes the unobserved transition to 159 keV. At this energy, a transition with multipolarity >1 and involving a parity change would be unobserved as our β-γ coincidence window was set at 500 ns. Therefore we are led to retain this last assumption and place the 546 keV transition decaying from the 705 keV level and followed by an unobservable 159 keV transition. Only a dedicated experiment can validate these conclusions.

Once we have the level scheme, the absolute γ intensities allow to determine the β branches and the corresponding log *ft* values (Table II). The intensity of the ground-state branch is obtained from the difference between $P_{0n}=(1-P_{1n}-P_{2n})$ and the sum of the feedings to γ-emitting levels. The quoted errors result mainly from the uncertainty of the estimated Q_β value [14] and the experimental intensities. From Table II, evidence is found for three allowed β transitions to 1243, 705 keV and g.s. of ^{33}Mg, the branch to the 1243 keV level being at the limit of the recommended range of allowed transitions [27].

In the decay scheme of Fig. 2, proposed J^π values result from β- and γ-decay selection rules and simple shell model configuration arguments. In this respect, the positive parity deduced from the allowed β branch to the ground state can be most easily explained with a two-particle–one-hole neutron state in ^{33}Mg resulting in $J^\pi=\frac{3}{2}^+$. The two other positive parity states populated by GT transitions are limited to $(\frac{1}{2}-\frac{7}{2})^+$ if we consider the two possible J^π values ($\frac{3}{2}^+$ and $\frac{5}{2}^+$) for ^{33}Na g.s. as resulting from the three particle configu-

TABLE III. Total β^- strength in each spin channel from the first two levels of ^{33}Na. The half-life obtained in these two cases has to be compared with the experimental one: 8.0(3) ms.

	$\frac{3}{2}^+$ ground state			$\frac{5}{2}^+$ ground state		
	$\frac{3}{2}^+ \rightarrow \frac{1}{2}^+$	$\frac{3}{2}^+ \rightarrow \frac{3}{2}^+$	$\frac{3}{2}^+ \rightarrow \frac{5}{2}^+$	$\frac{5}{2}^+ \rightarrow \frac{3}{2}^+$	$\frac{5}{2}^+ \rightarrow \frac{5}{2}^+$	$\frac{5}{2}^+ \rightarrow \frac{7}{2}^+$
S^- (GT units)	5.95	11.35	15.70	8.01	11.29	13.70
$T_{1/2}$ (ms)		2.70			2.76	

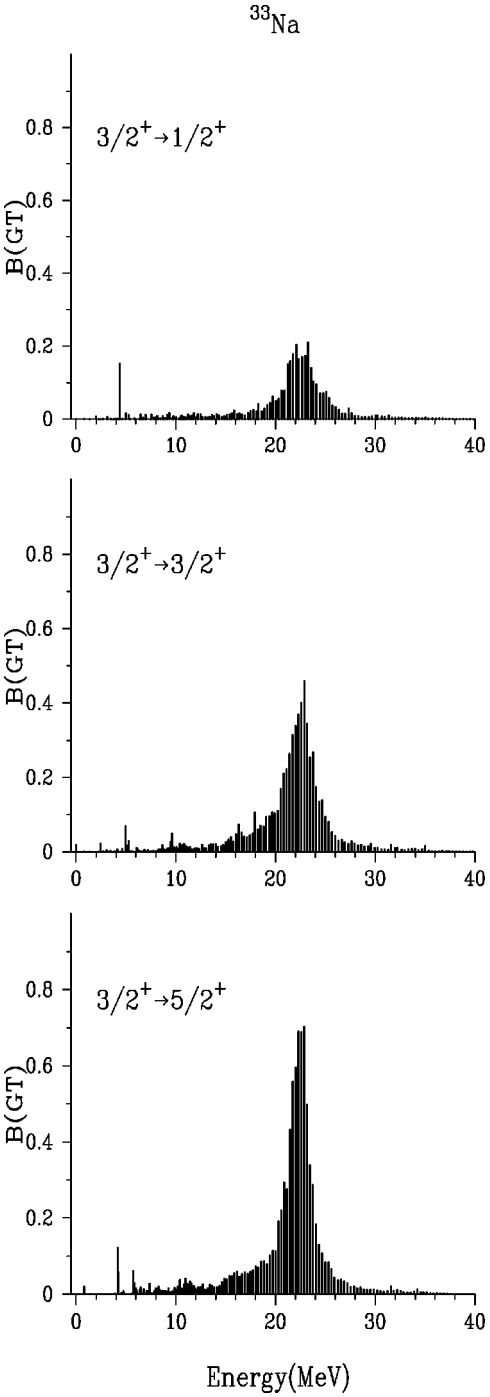

FIG. 5. β decay of ^{33}Na. Calculated values of Gamow-Teller strength distribution versus excitation energy in the final nucleus, assuming $\frac{3}{2}^+$ for ^{33}Na ground state.

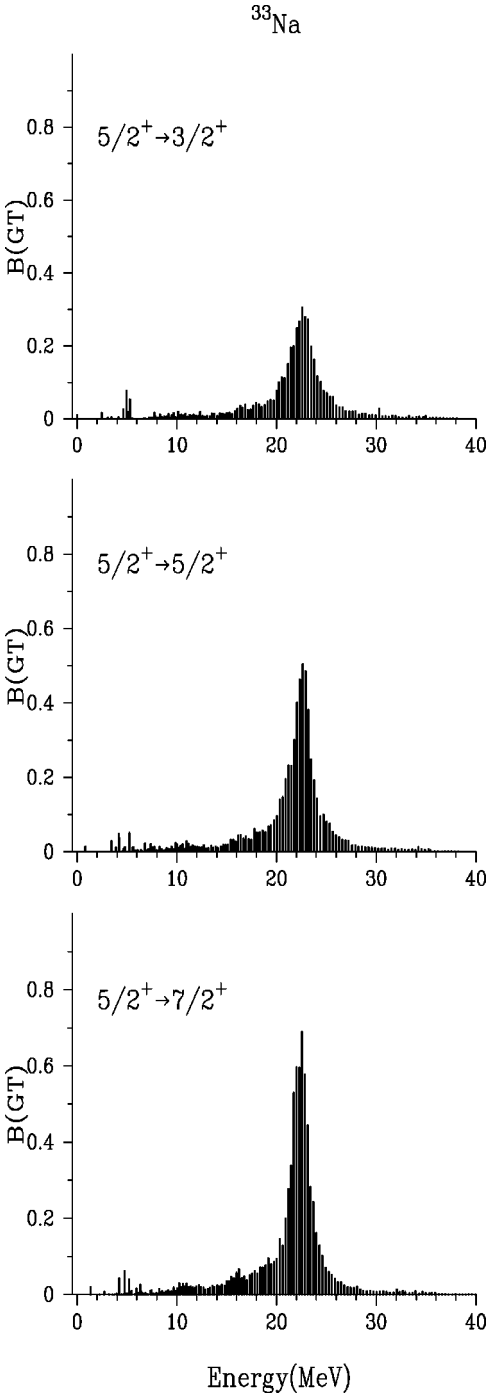

FIG. 6. β decay of ^{33}Na. Calculated values of Gamow-Teller strength distribution versus excitation energy in the final nucleus, assuming $\frac{5}{2}^+$ for ^{33}Na ground state.

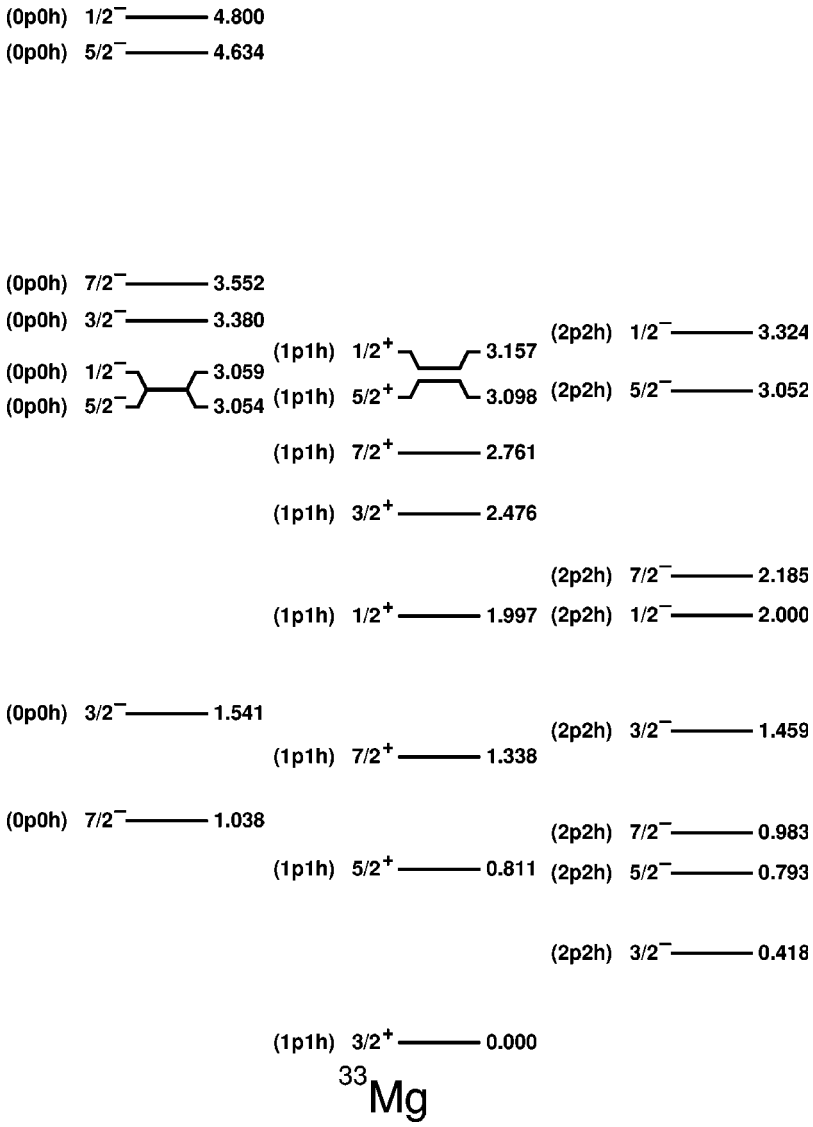

FIG. 7. Calculated low-lying states of ^{33}Mg: unmixed case.

ration, leading to a doublet of seniority.

For the negative parity states $J^{\pi}=\frac{7}{2}^{-}$ and $\frac{3}{2}^{-}$ are expected at low energy. The value proposed for $E_x=159$ keV($\frac{7}{2}^{-}$) and 484 keV($\frac{3}{2}^{-}$) are supported by the γ-ray results. According to the proposed level scheme, the 159 keV level decays by a long-lived, and therefore unobserved, $M2$ transition. For the 484 keV level, the $E1$ g.s. transition dominates completely the competing $E2$ branch to the 159 keV level. For the strongly β-populated 705 keV level, the three possible γ transitions are observed with comparable intensities, thus of the same multipole order. In our case, this order is restricted to dipoles as their decay time is short. In addition, dipoles to $\frac{3}{2}$ and $\frac{7}{2}$ levels fix $J^{\pi}=\frac{5}{2}^{+}$ to the 705 keV level. Finally, for the 1243 keV level, the lack of transitions to levels at 705 and 159 keV suggests $J^{\pi}=\frac{1}{2}^{+}$, the observed decay modes being then $M1$ and $E1$, respectively.

In the decay scheme (Fig. 2), we have also reported the main result of the analysis of the β-delayed neutrons, emitted in the ^{33}Na decay, and discussed in a separate paper [19]. Two strong peaks have been observed in the time-of-flight spectrum at $E_n=800(60)$ and 1020(80) keV and attributed to ^{33}Na decay with exclusion of the other delayed neutron emitters contributing to the spectrum (^{33}Mg, ^{32}Mg, and ^{33}Al). From our analysis [19], it appears that these neutrons populate the 2^+ state at 885 keV in ^{32}Mg locating around 4 MeV excitation energy in ^{33}Mg, the main part of the Gamow-Teller strength measured in this experiment.

IV. DISCUSSION

The β decay of ^{33}Na has been compared to shell model calculations. For n-rich $A=33$ nuclei, the situation is complicated since they are situated in the so-called island of inversion where many kinds of excitations $(0p0h,1p1h,2p2h)$ are coexisting. The discussion proceeds in three steps: first we discuss the nature of the parent nucleus ^{33}Na, then we analyze its beta decay and embed the final states produced by the shell model into the low-lying level spectrum observed for ^{33}Mg.

A. Shell model structure of ^{33}Na

Following our previous study of ^{34,35}Si [11], we work in the sd-pf valence space. Three different kind of excitations

are considered, $0\hbar\omega$, $1\hbar\omega$, and $2\hbar\omega$ and no mixing is assumed between $0\hbar\omega$ and $2\hbar\omega$ states. The interaction used is the one from Ref. [28], which was adjusted in our recent publication [11] to take into account the reduction of the gap between the $1f_{7/2}$ and $2p_{3/2}$ neutron orbitals in ^{35}Si. The calculated low-lying level spectrum of ^{33}Na is shown in Fig. 3. No ambiguity on the $0\hbar\omega$ nature of the ground state is seen. The first $1\hbar\omega$ and $2\hbar\omega$ states are lying around 1 MeV. Nevertheless, the first two states, $\frac{3}{2}^+$ and $\frac{5}{2}^+$ appear to be very close in energy. This degeneracy originates from the three protons in the the $1d_{5/2}$ orbital where the seniority 0 and 2 states coexist as can be already seen in the spectrum of ^{19}O. We will then consider both cases ($\frac{3}{2}^+$ and $\frac{5}{2}^+$) for the ground state in the discussion of the β decay.

B. Gamow-Teller β decay of ^{33}Na

The schematic decay of ^{33}Na is shown in Fig. 4. Two paths can be considered for the decay: one is to transform an *sd* neutron into an *sd* proton, the other is to transform an *fp* neutron into an *fp* proton. In both cases, the final state obtained in ^{33}Mg is a $1\hbar\omega$ excitation. But the important difference is that in the second case, the final state will be located at much higher excitation energy than in the first case. As we consider no sd-fp neutron excitations for the ^{33}Na ground-state, the β^- decay exhauts the full $3(N-Z)$ Ikeda sum rule, which amounts here to 33 GT units. Table III gives the B(GT) values in the different spin channels.

In Figs. 5 and 6 we show the detailed Gamow-Teller strength functions obtained with $J^\pi=\frac{3}{5}^+$ or $\frac{5}{2}^+$ as the ground states of ^{33}Na. The standard quenching factor of 0.77 [29] was used to renormalize the operator. In these figures no real distinction can be observed between the two spin-parity states. This is not surprising since both parent states are similar in nature. Both calculations show β decay branches to the ^{33}Mg ground-state, to the first $\frac{5}{2}^+$ state at 0.811 MeV and to a multiplet of states located around 4 MeV. This is in a full agreement with the experimental results exhibiting the strong β branches deduced from the delayed neutron measurement [19]. The computed half-lives are also very similar, 2.70 and 2.76 ms. The agreement with the experimental half-life can be considered fair since this observable is determined solely by the small fraction of the strength function leading to low-lying states. In particular, few states determining the half-life carry only a few percent of the whole strength and such an accuracy is evidently very difficult to achieve in the theoretical calculation.

C. The structure of ^{33}Mg within the shell model

Shell model calculations for the states of ^{33}Mg are shown in Fig. 7. The complexity of the spectrum is evident and derives from the coexistence of different kind of excitations. The key feature is indeed the nature of the ground state of this nucleus which is predicted to be a $J^\pi=\frac{3}{2}^+$ state resulting from a $1p1h$ excitation, i.e., a $2p1h$ configuration in this $N=21$ nucleus. This spin-parity value appears to be confirmed by the experiment. For the excited levels, the predicted coexistence is supported by the presence of many states at low energy. This relatively high number of states, compared to ^{35}Si, makes a one to one assignment difficult between the observed and the calculated states. Nevertheless, the main features of the ^{33}Na decay and the level structure of ^{33}Mg is understood. The drawback of the present calculation was the absence of mixing which was not taken into account for $0p0h$ and $2p2h$ configurations. In particular, the close proximity of $(\frac{7}{2}^-)_{1,2}$ states does not support such a strong approximation. Therefore, following the procedure previously applied to ^{34}Si [11], we performed a two by two mixing by calculating the nondiagonal matrix element between these fixed configurations. The resulting spectrum is shown is Fig. 8. The repulsion between the two $\frac{7}{2}^-$ states has split the degeneracy and lowered strongly the first $\frac{7}{2}^-$ level. This gives a theoretical candidate for the long-lived $M2$ isomer suggested by the present experiment (see Sec. III).

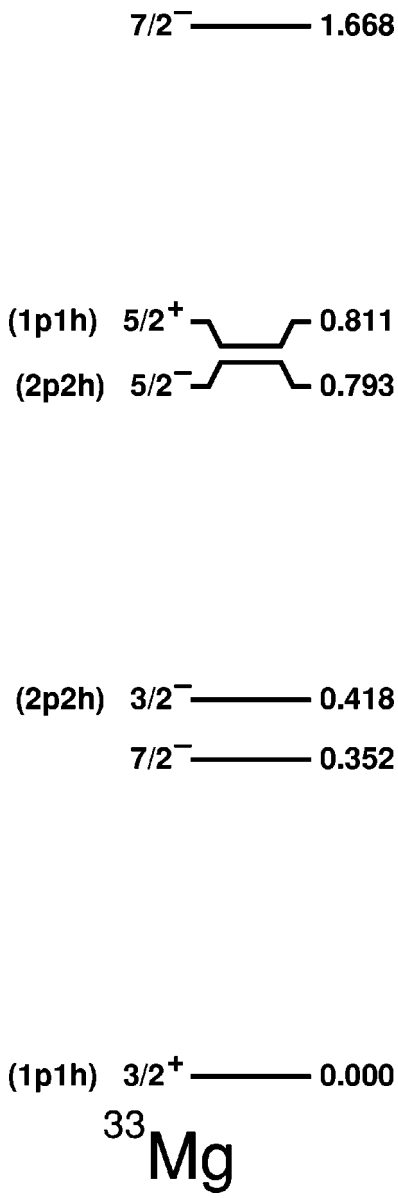

FIG. 8. Calculated low-lying states of ^{33}Mg with $\frac{7}{2}^-$ states after mixing.

In conclusion, the case of ^{33}Mg is of particular interest as it shows the first observation of inversion of states in this region. It provides a nice example of the selectivity of β decay measurements that can provide a direct model-independent evidence for a positive parity ground state of ^{33}Mg.

ACKNOWLEDGMENTS

This work was supported in part by the European Union Program of Training and Mobility in Research and in part by the IN2P3 (Institut National de Physique Nucléaire et de Physique des Particules).

[1] C. Thibault *et al.*, Phys. Rev. C **12**, 644 (1975).
[2] X. Campi, H. Flocard, A. K. Kerman, and S. Koonin, Nucl. Phys. **A251**, 193 (1975).
[3] B. H. Wildenthal and W. Chung, Phys. Rev. C **22**, 2260 (1980).
[4] A. Watt, R. P. Singhal, M. H. Storm, and R. R. Whitehead, J. Phys. G **7**, L145 (1981).
[5] A. Poves and J. Retamosa, Phys. Lett. B **184**, 311 (1987); Nucl. Phys. **A571**, 221 (1994).
[6] E. K. Warburton, J. A. Becker, and B. A. Brown, Phys. Rev. C **41**, 1147 (1990).
[7] R. W. Ibbotson *et al.*, Phys. Rev. Lett. **80**, 2081 (1998).
[8] B. V. Pritychenko *et al.*, MSU Research Report No. MSUCL-1156, 2000 (unpublished).
[9] B. V. Pritychenko *et al.*, MSU Research Report No. MSUCL-1157, 2000 (unpublished).
[10] F. Sarazin *et al.*, Phys. Rev. Lett. **84**, 5062 (2000).
[11] S. Nummela *et al.*, Phys. Rev. C **63**, 044316 (2001).
[12] D. Guillemaud *et al.*, Nucl. Phys. **A426**, 37 (1984).
[13] M. Langevin *et al.*, Nucl. Phys. **A414**, 151 (1984).
[14] G. Audi, O. Bersillon, J. Blachot, and A. H. Wapstra, Nucl. Phys. **A624**, 1 (1997).
[15] P. Möller, J. R. Nix, W. D. Myers, and W. J. Swiatecki, At. Data Nucl. Data Tables **59**, 185 (1995).
[16] H. Sakurai *et al.*, Phys. Rev. C **54**, 2802 (1996).
[17] O. Tarasov *et al.*, Phys. Lett. B **409**, 64 (1997).
[18] H. Sakurai *et al.*, Phys. Lett. B **448**, 180 (1999).
[19] Z. Radivojevic *et al.*, Nucl. Instrum. Methods Phys. Res. A (to be published)
[20] M. Bounajma, Ph.D. thesis, Strasbourg, 1996.
[21] C. Detraz *et al.*, Nucl. Phys. **A349**, 378 (1983).
[22] C. Detraz *et al.*, Phys. Rev. C **19**, 164 (1979).
[23] G. Klotz *et al.*, Phys. Rev. C **47**, 2502 (1993).
[24] M. Robinson *et al.*, Phys. Rev. C **53**, 1465 (1996).
[25] B. Fornal *et al.*, Phys. Rev. C **55**, 762 (1997).
[26] P. Baumann *et al.*, Phys. Rev. C **58**, 1970 (1998).
[27] S. Raman and N. B. Gove, Phys. Rev. C **7**, 1993 (1973).
[28] J. Retamosa, E. Caurier, F. Nowacki, and A. Poves, Phys. Rev. C **55**, 1266 (1997).
[29] B. H. Wildenthal, M. S. Curtin, and B. A. Brown, Phys. Rev. C **28**, 1343 (1983).